

Bis(imino)pyridine–Iron(II) Complexes for Ethylene Polymerization¹

Saman Damavandi^a, Gholam Hossein Zohuri^{b,*},
Reza Sandaroos^c, and Saeid Ahmadjo^{d,**}

^aResearch and Development Division, Rejal Petrochemical Co. Isfahan, Iran

^bDepartment of Chemistry, Faculty of Science, Ferdowsi University of Mashhad, Mashhad, Iran

^cDepartment of Chemistry, Faculty of Science, University of Birjand, Birjand, Iran

^dDepartment of Catalyst, Iran Polymer and Petrochemical Institute, Tehran, Iran

*e-mail: Zohuri@um.ac.ir

**e-mail: s.ahmadjo@ippi.ac.ir

Received June 7, 2016;

Revised Manuscript Received September 29, 2016

Abstract—Ethylene polymerization was carried out using new late transition metal 2,6-bis(imino)pyridine catalysts containing different substituents (H, NO₂, and OCH₃) at the para position of the pyridine ring, activated by methylaluminoxane. Effects of polymerization parameters such as ethylene pressure, reaction temperature, hydrogen concentration and structure variation on the catalysts activities and polymer properties were investigated. Introducing the functionality in the para-position of the pyridine ring of the catalysts had remarkable effect on the polymer properties as well as the catalysts activities.

DOI: 10.1134/S1560090417010031

INTRODUCTION

Since the first reports of active catalysts for ethylene polymerization based on iron and cobalt supported by bis(imino)pyridine ligands (BIMP) [1, 2], there have been numerous studies directed at modifying the bis(imino)pyridine frame [3–15] especially by the groups attached to the imine nitrogen donors [6–12]. Bennett reported the imidazolyl based catalyst [16]. Gibson studied the effect of different substitutes in the imine carbon position on catalyst activity [17]. Guo has synthesized unsymmetrical iron(II) bis(imino)pyridyl catalysts for ethylene polymerization and has investigated the effect of the bulky *ortho* substituent [18]. Besides, various bis(imino)pyridine iron(II) catalysts are generally used for production of linear polyethylenes with broad and bimodal molecular weight distribution [18–20]. Therefore, great deal of researchers is involved in the design of new ligands, changing the backbone substituents on the carbon atoms of imine groups and replacing the aniline moiety and in the study of their activity in ethylene polymerization. However, the introducing functional groups to the pyridine ring of the ligands is less studied.

As a part of our ongoing research [21–24], herein, ethylene polymerization mediated by new

bis(imino)pyridine catalysts (Scheme 1) in the different polymerization conditions was investigated.

EXPERIMENTAL

Materials

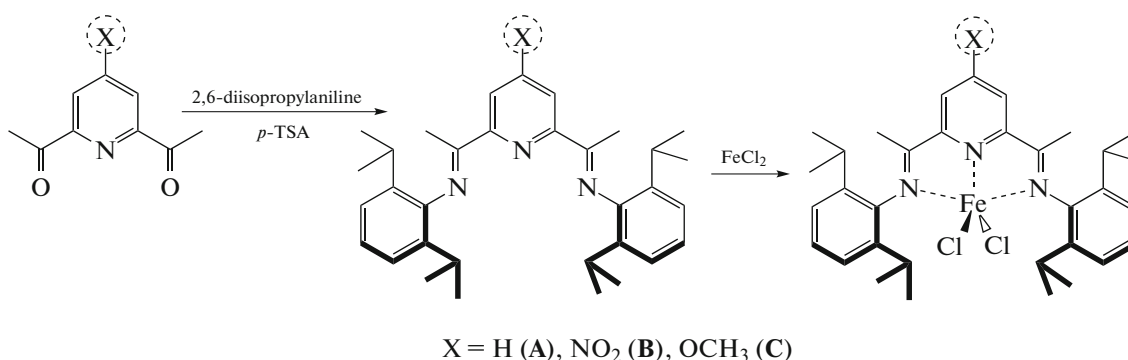
Methylaluminoxane (MAO, 10%), 2,6-diisopropylaniline and other chemicals were purchased from Sigma-Aldrich Chemical Co. 2,6-Diacetylpyridine (purity > 99%) was supplied by Acros (Somerville, NJ). For polymerization, MAO was added to the reactor previously purged with argon for 15 min and containing toluene, following by addition of the catalyst in dissolved dichloromethane (5 mL) and ethylene. The content was stirred and maintained under ethylene throughout the polymerization. The solid polyethylene (PE) was collected by filtration, washed with acidic methanol (50 mL) and dried in the vacuum oven.

Characterization

All manipulations were carried out under an atmosphere of nitrogen using standard Schlenk techniques. Solvents were stored over sodium wire and 13X and 4 Å activated types molecular sieves.

Differential scanning calorimetry (Universal V4IDTA) was carried out with a rate of 10 grad/min, 30 mL/min of ultra pure nitrogen gas was fed contin-

¹ The article is published in the original.



Scheme 1.

uously to purge the calorimeter. The polymer sample, about 5 mg, was first equilibrated at 30°C, and then heated up to 180°C. The peak temperature with the highest endotherm was chosen as the melting point. Degree of crystallinity of a polyethylene sample was calculated according to our previous report [23].

Elemental analysis for was carried out by CHNO type Thermo Firingan 11112EA microanalyzer. ¹H NMR spectra were recorded on a Bruker AC-400 spectrometer at 293 K. The viscosity average molecular weight (M_v) of some polymer samples was determined according to the literature [24]. Intrinsic viscosity $[\eta]$ was measured in decaline at $135 \pm 1^\circ\text{C}$ using an Ubbelohde suspended level dilution viscometer. M_v values were calculated through Mark-Houwink $\eta = M_v K^\alpha$ equation ($\alpha = 0.7$, $K = 6.2 \times 10^{-4}$) [22].

Ligand and Catalyst Preparation

4-Nitro-2,6-diacetylpyridine and 4-methoxy-2,6-diacetylpyridine were synthesized according to our previous work [21]. 4-Nitro-2,6-diacetylpyridine: ¹H NMR (CDCl₃, δ_H , ppm): 8.69 (s, 2H), 2.54 (s, 6H). Anal. (C₉H₉NO₂), %: C, 66.25; H, 5.56; N, 8.58. Found, %: C, 65.99; H, 5.50; N, 8.52. 4-Methoxy-2,6-diacetylpyridine: ¹H NMR (CDCl₃, δ_H , ppm): 7.69 (s, 2H), 3.72 (s, 3H), 2.51 (s, 6H). Anal. (C₁₀H₁₁NO₃), %: C, 62.17; H, 5.74; N, 7.25. Found, %: C, 61.95; H, 5.71; N, 7.19.

2,6-Diacetyl pyridine bis(2,6-diisopropylphenylimine) (a): 2,6-Diisopropylaniline (12.4 mmol, 2.38 mL) and p-toluenesulfonic acid were added to the solution of 2,6-diacetylpyridine (6.1 mmol). The resulting mixture was stirred at 25°C for 2 days until the precipitate formed. The white precipitate was filtered, washed with methanol and dried. A pale yellow solid was obtained. The resulting solid was dissolved in chloroform, then excess of 2,6-diisopropylaniline (6.1 mmol) was added to solution. The solution was refluxed for 5 days. The solvent was removed, a yellow powder was obtained, washed with *n*-hexane and

dried. ¹H NMR (CDCl₃, δ_H , ppm): 1.2 (d, 24H), 2.3 (s, 6H), 2.8 (m, 4H), 7–7.2 (m, 6H), 7.88 (t, 1H), 8.4 (d, 2H). Anal. (C₃₃H₄₃N₃), %: C, 82.32; H, 8.94; N, 8.73. Found, %: C, 82.33; H, 9.11; N, 8.68.

4-Nitro-2,6-diacetyl pyridine bis(2,6-diisopropylphenylimine) (b): The similar procedure was used for synthesis of compound (b). The product was isolated as an orange solid. ¹H NMR (CDCl₃, δ_H , ppm): d, 8.70 (s, 2H), 7.25–6.85 (m, 6H), 3.02 (m, 4H), 2.25 (s, 6H), 1.2 (d, 24H). Anal. (C₃₃H₄₂N₄O₂), %: C, 75.25; H, 8.04; N, 10.64. Found, %: C, 74.86; H, 8.11; N, 10.44.

4-Methoxy-2,6-diacetyl pyridine bis(2,6-diisopropylphenylimine) (c): The similar procedure was used for synthesis compound (c), which was obtained as a pale brown solid. ¹H NMR (CDCl₃, δ_H , ppm): d, 7.42 (s, 2H), 7.20–6.80 (m, 6H), 3.65 (s, 3H), 3.10 (m, 4H), 2.25 (s, 6H), 1.25 (d, 24H). Anal. (C₃₃H₄₅N₃O), %: C, 79.80; H, 8.86; N, 8.21. Found, %: C, 79.27; H, 8.93; N, 8.27.

Catalyst Synthesis

[2,6-diacetylpyridinebis(2,6-diisopropylphenylimine)] iron(II) dichloride (A). In a dry, oxygen free atmosphere, FeCl₂ (anhydrous, 1.078 mmol) was dissolved in dry THF, then 1.156 mmol of ligand (a) was added to this solution. The mixture was stirred for 3 days at 25°C and a dark blue precipitate was formed. The solid was filtered, washed with dry *n*-hexane and dried under nitrogen. The solid catalyst of [2,6-diacetylpyridinebis(2,6-diisopropylphenylimine)] iron(II) dichloride (A) was obtained in a yield of 78%. ¹H NMR (CD₂Cl₂, broad singlets are observed in each case, δ_H , ppm): -20.18 (s, 6H), 12.60 (24H), 15.12 (4H), 20.37 (6H), 38.58 (1H), 80.25 (2H). Anal. (C₃₃H₄₃Cl₂FeN₃), %: C, 65.14; H, 7.12; N, 6.91%. Found, %: C, 64.31; H, 7.22; N, 6.88.

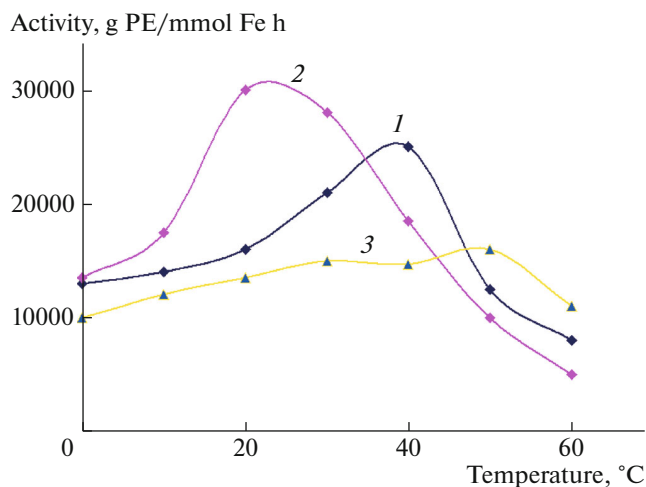


Fig. 1. (Color online) Effect of the temperature on the average rate of polymerization for catalysts (1) A, (2) B, and (3) C. Polymerization conditions: time 60 min, monomer pressure 5 bar, $[Al] : [Fe] = 1000 : 1$, $[Fe] = 0.35 \times 10^{-3}$ mmol.

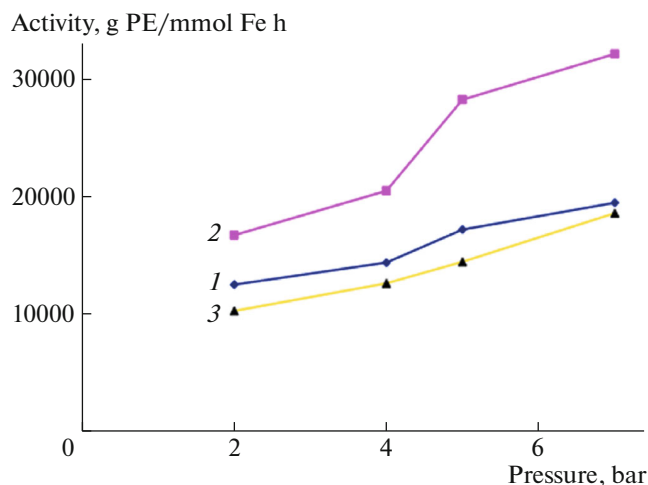


Fig. 2. (Color online) Effect of monomer pressure on the average rate of polymerization for catalysts (1) A, (2) B, and (3) C. Polymerization conditions: $T = 30^\circ\text{C}$, time 60 min, $[Al] : [Fe] = 1000 : 1$, $[Fe] = 0.35 \times 10^{-3}$ mmol.

[4-Nitro-2,6-diacetylpyridinebis(2,6-diisopropylphenylimine)] iron(II) dichloride (B). By using the same procedure, catalyst (B) was obtained in 76% yield as a blue solid. $^1\text{H NMR}$ (CD_2Cl_2 , broad singlets are observed in each case, δ_{H} , ppm): -21.23 (s, 6H), 12.52 (24H), 15.03 (4H), 20.25 (6H), 39.22 (1H), 80.05 (2H). Anal. ($\text{C}_{33}\text{H}_{42}\text{Cl}_2\text{FeN}_4\text{O}_2$), %: C, 60.65; H, 6.48; N, 8.57%. Found: C, 60.28; H, 6.33; N, 8.49.

[4-Methoxy-2,6-diacetylpyridinebis(2,6-diisopropylphenylimine)] iron(II) dichloride (C). By using the same procedure, catalyst (C) was obtained in 75% yield as a blue solid. $^1\text{H NMR}$ (CD_2Cl_2 , broad singlets are observed in each case, δ_{H} , ppm): -21.28 (s, 6H), 12.45 (24H), 15.01 (4H), 20.23 (6H), 40.13 (1H), 81.01 (2H). Anal. $\text{C}_{34}\text{H}_{45}\text{Cl}_2\text{FeN}_3\text{O}$, %: C, 63.96; H, 7.10; N, 6.58%. Found, %: C, 63.48; H, 7.19; N, 6.51.

RESULTS AND DISCUSSION

The main purpose of this work is to study the effect of chemical nature of substituent at the *para*-position of the pyridine ring on the catalyst activity and polymer properties. Replacing the *para*-proton of pyridine ring of the ligand with NO_2 and methoxy substituents (B and C) has a dramatic effect on catalyst performance (Scheme 1). However, all three catalysts exhibited high activity for ethylene polymerization at low and high pressure runs. The catalysts gave the activities in the order of: $\text{B} > \text{A} > \text{C}$.

For all the three catalysts, the effect of reaction temperature and ethylene pressure on catalyst activity was studied. The influence of polymerization temperature on activity was investigated at the range of the temperatures 10 – 60°C , while the $[Al]/[Fe]$ molar ratio was kept constant at $1000:1$.

As it can be seen in Fig. 1, the highest productivity of the catalysts A, B and C was achieved at about 40 , 25 and 50°C respectively. Activity of catalyst A increased with the polymerization temperature up to 40°C , but at higher polymerization temperatures it decreased due to the increase in catalyst deactivation rate known for most of olefin polymerization catalysts. The effect of polymerization temperature on catalyst activity might be explained by Brookhart theory on deactivation mechanism of α -diimine catalysts [25, 26]. The motion and rotation of aryl ring is increased at higher polymerization temperature. Therefore, due to the C–H bond activation of an *ortho* alkyl substituent, perturbation occurred in coordination step through a disorder in overlap of empty *d* orbital of the metal center with π -olefin orbital, leads to reduction of the activity of active centers [27]. The thermal stability of catalyst C was higher than of other catalysts probably due to *p*- OCH_3 substitution of the pyridine ring. However, its overall activity was lower. Catalyst B with *p*- NO_2 substitution showed the highest activity in the polymerization at 20°C . However at higher polymerization temperature its activity decreased.

The effect of ethylene pressure on catalysts activities followed the same trend for all three catalysts (Fig. 2). The catalyst activity increased with ethylene pressure, which is expected since catalyst active sites are exposed to higher ethylene concentration at higher pressure.

Ethylene polymerization was carried out using different amount of hydrogen as a chain transfer agent. As it can be seen in Fig. 3, higher amount of hydrogen could increase the activity of the catalysts A and C slightly, while H_2 did not affect the activity of the catalyst B. 2,1-Reinsertion of short olefin branches, are

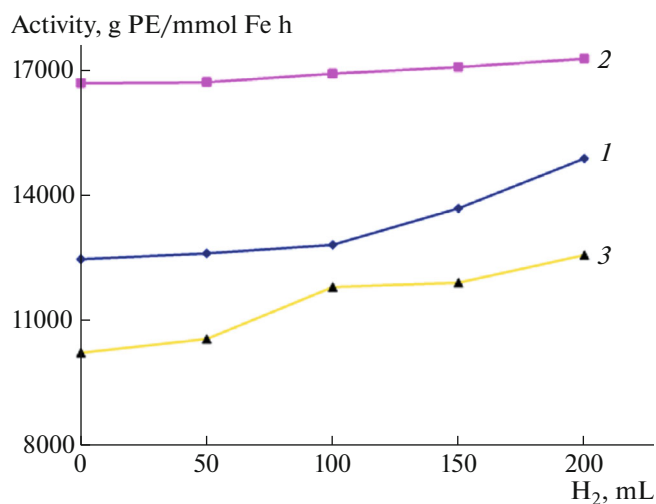


Fig. 3. (Color online) Effect of hydrogen on the average rate of polymerization for catalysts (1) A, (2) B, and (3) C. Polymerization conditions: time 60 min, monomer pressure 2 bar, [Al] : [Fe] = 1000 : 1, [Fe] = 0.35×10^{-3} mmol, $T = 30^\circ\text{C}$.

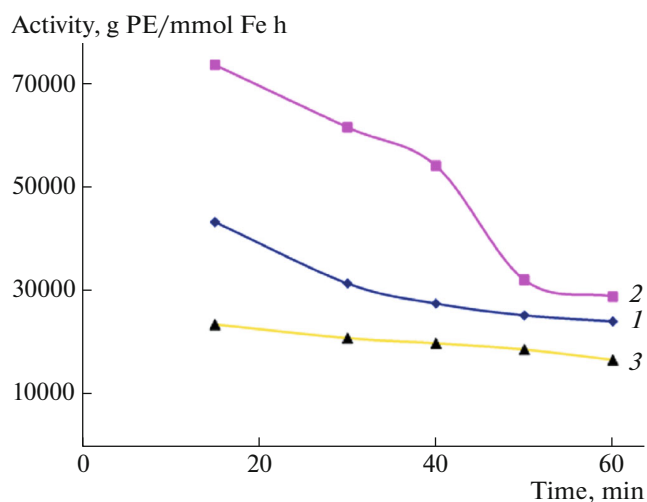


Fig. 4. (Color online) Time dependences of the catalytic activities of catalysts (1) A, (2) B, and (3) C at 40, 25 and 30°C respectively. Polymerization conditions: monomer pressure 5 bar, [Al] : [Fe] = 1000 : 1, [Fe] = 0.35×10^{-3} mmol.

still capable to be coordinated to the catalyst centers, is probable. [26, 27]. We have recently proposed a reasonable mechanism for reactivation of active centers by hydrogen resulting in an increase in activity [22].

With the aid of Gaussian software (09) using B3LYP method of theory with the Lan12dz basis set [28] the conformations and QEq charges of catalysts A–C were calculated. It is worth noting that QEq is only focused on the electronic effects. Although electronic and steric effects will change together when a substituent is changed, owing to the almost similar bulky hindrance, the interference of steric effect is reduced. A comparison between the activity and QEq charge showed in Table 1. A good match between the sequence of QEq charges and electron-withdrawing abilities was observed. For example, the nitro group is electron-poorer than the other moieties, leading to a more electrophilic metal center, i.e. a higher charge value for Fe. The relationship between activity and net charge of the central metal atom thus is the following. The higher is the charge, the higher is the activity, which is different from those for early transition metal systems.

Table 1. Correlation between catalyst activities and catalyst charges

Catalyst	Activity, g PE/mmol Fe.h	QEq charge on Fe
A	34.3	0.375
B	56.2	0.397
C	28.5	0.334

Figure 4 showed the time dependences of catalytic activities of catalysts for ethylene polymerizations at optimum polymerization temperature obtained for each catalyst. For the catalyst B which is the most active catalyst between the examined ones, catalytic activities decreased and the rate profile exhibited decay kinetic. Although the rate profile of catalysts A and C exhibited decay kinetic as the time increased, they displayed almost slower decay relative to that of catalyst B. As can be seen, the activities become stable from 30 to 60 min. It can be concluded that the electron-donating substituent attached to the *para*-position of the pyridine ring, can restrain the catalytically active iron centers from deactivation and effectively prolong the catalyst lifetime.

By change in the substitutions at the *para*-position of the pyridine ring in the catalysts, the polymers properties changed (Table 2). As expected, increasing the reaction temperature resulted in decreasing of the M_v of PE. It is noteworthy to mention that the M_v of PE changes in the range of catalysts in the order of $A > B > C$. The obtained polyethylene has a melting point at about $125\text{--}135^\circ\text{C}$ and crystallinity of about 48–65%. Higher pressure increased both the crystallinity and the M_v values of the obtained polymer.

CONCLUSIONS

The different *para* substituents (H, NO_2 , OCH_3) exhibit not significant effect on steric bulk of catalysts, but the electronic effects can provide different catalyst activities and polymers properties. The electronic effects of the *para* substituent of the pyridine moiety of the catalysts distinctly affect the molecular weights of the obtained polyethylenes. Catalyst A provides the

Table 2. Some characterization of the resulted polyethylene

Sample	Pressure, bar	Temperature, °C	Crystallinity, %	M_v	T_m , °C	PDI
(cat. A)	2	30	62	4.5×10^5	132	–
(cat. A)	4	30	60	5.1×10^4	130	7.4
(cat. A)	7	30	60	5.5×10^5	135	7.8
(cat. A)	7	50	57	4.7×10^5	130	–
(cat. B)	4	30	60	4.3×10^4	132	6.8
(cat. B)	4	50	55	4.1×10^4	125	–
(cat. B)	7	30	58	4.5×10^4	131	7.1
(cat. C)	4	30	62	3.5×10^4	125	8.1
(cat. C)	7	30	65	3.7×10^4	130	8.8
(cat. C)	8	30	48	3.9×10^4	130	–
(cat. C)	5	50	53	3.3×10^4	127	–

highest molecular weight of polyethylene among the prepared catalyst. In addition, lower thermal stability is observed for the catalyst **B** whereas the activity of the catalyst **C** toward increasing the polymerization temperature is surprisingly stable. Hydrogen slightly increases the activities of the catalysts **A** and **C**.

REFERENCES

- G. J. P. Britovsek, V. C. Gibson, B. S. Kimberley, P. J. Maddox, S. J. McTavish, G. A. Solan, A. J. P. White, and D. J. J. Williams, *Chem. Commun.* **7**, 849 (1998).
- B. L. Small, M. Brookhart, and A. M. A. Bennett, *J. Am. Chem. Soc.* **120**, 4049 (1998).
- Y. Chen, R. Chen, C. Qian, X. Dong, and J. Sun, *Organometallics* **22**, 4312 (2003).
- Y. F. Chen, C. T. Qian, and J. Sun, *Organometallics* **22**, 1231 (2003).
- G. J. P. Britovsek, V. C. Gibson, B. C. Kimberley, S. Mastroianni, R. Redshaw, G. A. Solan, A. J. P. White, and D. J. J. Williams, *Dalton Trans.* **10**, 1639 (2001).
- A. S. Abu-Surrah, K. Lappalainen, U. Piironen, P. Lehmus, T. Repo, and M. Leskela, *J. Organomet. Chem.* **648**, 55 (2002).
- M. E. Blum, C. Folli, and M. Doring, *J. Mol. Catal. A: Chem.* **212**, 13 (2004).
- C. Amort, M. Malaun, A. Krajete, H. Kopacka, K. Wurst, M. Christ, D. Lilge, M. O. Kristen, and B. Bildstein, *Appl. Organomet. Chem.* **16**, 505 (2002).
- Z. Ma, H. Wang, J. Qiu, D. Xu, and Y. Hu, *Macromol. Rapid Commun.* **22**, 1280 (2001).
- A. S. Ionkin, W. J. Marshall, D. J. Adelman, B. B. Fones, B. M. Fish, and M. F. Schiffrhauer, *Organometallics* **25**, 2978 (2006).
- V. C. Gibson, N. J. Long, P. J. Oxford, A. J. P. White, and D. J. Williams, *Organometallics* **25**, 1932 (2006).
- T. M. Smit, A. K. Tomov, V. C. Gibson, A. J. P. White, and D. J. Williams, *Inorg. Chem.* **43**, 6511 (2004).
- F. A. R. Kaul, G. T. Puchta, H. Schneider, F. Bielert, D. Mihalios, and W. A. Herrmann, *Organometallics* **21**, 74 (2002).
- K. Nomura, W. Sidokmai, and Y. Imanishi, *Bull. Chem. Soc. Jpn.* **73**, (2000).
- S. Al-Benna, M. J. Sarsfield, M. Thornton-Pett, D. L. Ormsby, P. J. Maddox, P. Bres, and M. Bochmann, *Dalton Trans.* **23**, 4247 (2000).
- A. M. A. Bennett, WO Patent No. 9827124 (1998).
- S. McTavish, G. J. P. Britovsek, T. M. Smit, V. C. Gibson, A. J. P. White, and D. J. Williams, *J. Mol. Catal. A: Chem.* **261**, 293 (2007).
- L. H. Guo, H. Y. Gao, L. Zhang, F. M. Zhu, and Q. Wu, *Organometallics* **29**, 2118 (2010).
- R. Renan-Cariou and J. W. Shabaker, *ACS Catal.* **5**, 4363 (2015).
- Olefin Upgrading Catalysis by Nitrogen-Based Metal Complexes II*, Ed. by J. Campora and G. Giambastiani (Springer, Dordrecht, 2011), Vol. 36.
- G. H. Zohuri, S. M. Seyedi, R. Sandaroos, S. Damavandi, and A. Mohammadi, *Catal. Lett.* **140**, 160 (2010).
- S. Ahmadjo, G. H. Zohuri, S. Damavandi, and R. Sandaroos, *React. Kinet., Mech. Catal.* **101**, 429 (2010).
- G. H. Zohuri, S. Damavandi, R. Sandaroos, and S. Ahmadjo, *Polym. Bull.* **66**, 1051 (2010).
- R. Sandaroos, S. Damavandi, and A. Farhadipour, *Macromol. Chem. Phys.* **211**, 2339 (2010).
- K. Allen, J. Campos, O. Daugulis, and M. Brookhart, *ACS Catal.* **5** (1), 456 (2015).

26. *Late Transition Metal Polymerization Catalysis*, Ed. by B. L. Rieger, B. L. Saunders, S. Kacker, and S. Striegler, (Wiley-VCH, Weinheim, 2003).
27. S. Damavandi, N. Samadieh, S. Ahmadjo, Z. Etemadinia, and G. H. Zohuri, *Eur. Polym. J.* **64**, 118 (2015).
28. M. J. Frisch, G. W. Trucks, H. B. Schlegel, G. E. Scuseria, M. A. Robb, J. R. Cheeseman, G. Scalmani, V. Barone, B. Mennucci, G. A. Petersson, H. Nakatsuji, M. Caricato, X. Li, H. P. Hratchian, A. F. Izmaylov, J. Bloino, G. Zheng, J. L. Sonnenberg, M. Hada, M. Ehara, K. Toyota, R. Fukuda, J. Hasegawa, M. Ishida, T. Nakajima, Y. Honda, O. Kitao, H. Nakai, T. Vreven, J. A. Montgomery, J. E. Peralta, F. Ogliaro, M. Bearpark, J. J. Heyd, E. Brothers, K. N. Kudin, V. N. Staroverov, R. Kobayashi, J. Normand, K. Raghavachari, A. Rendell, J. C. Burant, S. S. Iyengar, J. Tomasi, M. Cossi, N. Rega, N. J. Millam, M. Klene, J. E. Knox, J. B. Cross, V. Bakken, C. Adamo, J. Jaramillo, R. Gomperts, R. E. Stratmann, O. Yazyev, A. J. Austin, R. Cammi, C. Pomelli, J. W. Ochterski, R. L. Martin, K. Morokuma, V. G. Zakrzewski, G. A. Voth, P. Salvador, J. J. Dannenberg, S. Dapprich, A. D. Daniels, Ö. Farkas, J. B. Foresman, J. V. Ortiz, J. Cioslowski, and D. J. Fox, *Gaussian 09*, Revision A.02, (Gaussian, Inc., Wallingford CT, 2009).